Scheme I

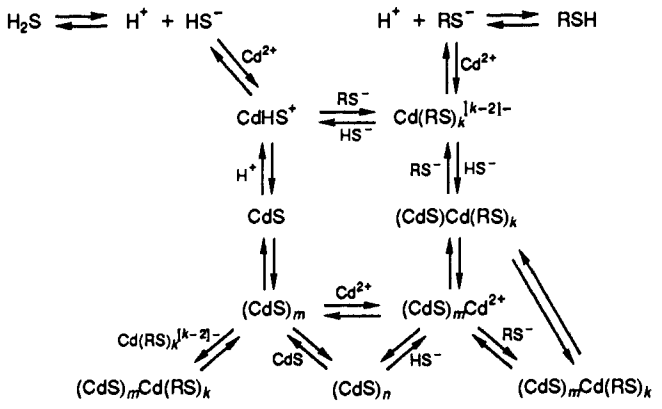

dilution of the solution prior to deposition on the grids or by further addition of external stabilizers. Diffraction patterns for all preparations show the cubic β-CdS structure. Results from EDAX experiments are shown in Figure 9, where the ratio of sulfur/cadmium signals from specimens deposited following irradiation at pH 7.1 and 4.3 are compared with those of a specimen deposited from chemical preparation of CdS in the absence of RSH. It is clear from Figure 9 that the sample prepared at pH 4.3 is slightly enriched in sulfur while the one prepared at pH 7.1 indicates substantial increase in sulfur content. This is in accordance with the above discussion where the sulfur-to-cadmium ratio may be expected to increase due to complexation of thiolate at the surface.

Conclusions

The essential features of the mechanism for CdS growth, controlled by RS^-, which emerges from this study, are outlined in Scheme I. The end products at the bottom right and left sides of the scheme represent the CdS core with the cadmium–thiolate complexes covalently bound to the surface. The subscript k is used to indicate the possibility of polynuclear complex formation with both free Cd^{2+} ions in solution and at the surface. The effect of pH appears through the acid–base equilibria of H_2S and RSH. The important step for control of the growth is provided by the competition between RS^- and HS^- for the Cd^{2+} ions at the surface of the growing particle. The left-side branch of the scheme dominates at low pHs when thiolate complexation of free Cd^{2+} is minimal. The right side dominates at higher pHs and includes the growth of CdS clusters bound to the polynuclear complexes.

Two main advantages of the thiolate controlled growth can be indicated at this point. The ability to externally control the growth and the final size of the particles simply by adjusting the relative $Cd^{2+}/RSH/H_2S$ concentrations is one obvious appealing feature. No less significantly is the ability to control, and modify, the surface properties of the particles through use of a variety of derivatized thiols in such systems. It is the strong binding of the cadmium ions to both the CdS lattice and the thiol that provides this route for surface modification. Interestingly the recent observation of cadmium bio-mineralization in the form of CdS probably operates via a similar mechanism.[20]

Acknowledgment. The dedicated operation of the linac by D. Ficht and G. Cox is much appreciated. This work was performed under the auspices of the Office of Basic Energy Sciences, Division of Chemical Science, US-DOE, under contract No. W-31-109-ENG-38.

(20) (a) Dameron, C. T.; Reese, R. N.; Mehra, R. K.; Kortan, A. R.; Carroll, P. J.; Steigerwald, M. L.; Brus, L. E.; Winge, D. R. *Nature* **1989**, *338*, 596. (b) Reese, R. N.; Winge *J. Biol. Chem.* **1988**, *263*, 12832.

Synthesis, Luminescence, and Excited-State Complexes of the Tris(1,10-phenanthroline)- and Bis(terpyridine)iridium(III) Cations

N. P. Ayala,[1] C. M. Flynn, Jr.,[2] LouAnn Sacksteder,[3] J. N. Demas,*[,3] and B. A. DeGraff*[,4]

Contribution from the Departments of Chemistry, University of Virginia, Charlottesville, Virginia 22901, and James Madison University, Harrisonburg, Virginia 22807.
Received September 18, 1989

Abstract: We report the synthesis and luminescence properties of $Ir(phen)_3^{3+}$ and $Ir(terp)_2^{3+}$ (phen = 1,10-phenanthroline and terp = 2,6-bis(2-pyridyl)pyridine). Their emissions are assigned to predominantly π–π^* phosphorescences. A novel excited-state complex is proposed to form between $Ir(phen)_3^{3+}$ and $Ir(terp)_2^{3+}$ and $HgCl_2$. Although $HgCl_2$ is normally a quencher, it can greatly enhance the lifetimes and luminescence efficiencies of the $Ir(phen)_3^{3+}$ and $Ir(terp)_2^{3+}$—up to an order of magnitude. The changes arise from alteration of the radiative and nonradiative rate constants in the excited-state complex. The effect of temperature, solvent, oxygen, and inert ions on the interactions of $HgCl_2$ with the excited complexes is explored. A simple associative model accurately reproduces all lifetime and intensity changes. A rationale based on the well-known affinity of $HgCl_2$ for aromatic molecules is proposed.

The photochemistry and photophysics of platinum metal complexes have played a pivotal role in attempts to develop new solar energy conversion and photocatalytic systems.[5] Among this group, the complexes of Ir(III) with α-diimine ligands have particularly complex chemistry and photophysics.[6-9] In particular, $Ir(bpy)_3^{3+}$

(1) Current affiliation: Westwood Chemical Corp., Middeltown, NY 10940.
(2) Current affiliation: U.S. Bureau of Mines, Reno, NV.
(3) University of Virginia.
(4) James Madison University.

(5) (a) *Energy Resources through Photochemistry and Catalysis*; Grätzel, M., Ed.; Academic Press: New York, 1983. (b) Kalyanasundaram, K. *Coord. Chem. Rev.* **1982**, *46*, 159. (c) Balzani, V.; Bolletta, F.; Gandolfi, M. T.; Maestri, M. *Top. Curr. Chem.* **1978**, *75*, 1. (d) Kalyanasundaram, K. *Photochemistry in Microheterogeneous Systems*; Academic Press, 1987.
(6) DeArmond, M. K.; Carlin, C. M. *Coord. Chem. Rev.* **1981**, *36*, 325.

0002-7863/90/1512-3837$02.50/0

and $Ir(phen)_3^{3+}$ (bpy = 2,2'-bipyridine and phen = 1,10-phenanthroline) have not been widely studied since they are difficult to prepare in high purity and are photosensitive.[8-10]

Charge-transfer and other excited-state interactions such as exciplexes are well studied in organic systems. Only recently have excited-state Lewis acid–base interactions been demonstrated for platinum metal complexes. The nature and scope of these interactions is poorly delineated due to the paucity of examples.[11] Recently, systems displaying exciplex behavior based on the interactions of silver ions with Ru(II) complexes have been reported.[11b-d] Other systems have involved $Pt_2(P_2O_5H_2)^{4-}$ and Tl^+,[11e] Also Cu^+–phenanthroline complexes show quenching by Lewis bases attributed to exciplex-like intermediates.[11f,g] In iridium systems, both nonemissive and emissive exciplexes have been inferred for $*Ir^{(III)}(C^3,N'\text{-bpy})(bpy)_2^{2+}$ with Br^-.[12] An exciplex has been suggested as the key intermediate in the catalyzed valence isomerization of substituted norbornadienes.[13] Interestingly, the manifestation of these interactions has been quite diverse.

All of the prior emitting systems have exhibited classical exciplex behavior with a pronounced red shift and usually a pronounced decrease in, or elimination of, luminescence. We report on systems that do not follow the typical pattern. Excited-state complex formation can greatly increase luminescence efficiencies and lifetimes; in addition there are no pronounced spectral shifts. Our systems demonstrate that suitable inorganic systems can be longer lived and more highly luminescent than the parent complexes; this makes for easier monitoring of excited-state interactions and easier scavenging of excited-state energy in bimolecular processes.

We report the synthesis of the previously unknown $Ir(terp)_2^{3+}$ (terp = 2,6-bis(2-pyridyl)pyridine) and of spectroscopically pure $Ir(phen)_3^{3+}$. As an extension of our work on the Hg(II)/Hg(I) energy storage system,[14] we examined $HgCl_2$ quenching. Surprisingly, we found a novel excited-state interaction between $HgCl_2$ and Ir(III)–α-diimine complexes in MeCN, DMF, and MeOH that we fully characterize. In MeCN and DMF, $HgCl_2$ forms highly emissive species with $Ir(phen)_3^{3+}$ and $Ir(terp)_2^{3+}$ that have longer lifetimes and higher quantum yields than the parent complexes. Emissive excited-state complexes are formed in MeOH, but these have shorter lifetimes and smaller quantum yields than the parent complexes.

Experimental Section

Materials. Spectrograde acetonitrile (MeCN), and *N,N'*-dimethylformamide (DMF), and methanol (MeOH) were from Aldrich. Bulk grade dichloromethane (CH_2Cl_2), butyronitrile (BuCN), and propionitrile (PrCN) from Fischer Scientific were redistilled and stored over molecular sieves to remove traces of water.

$K_3IrCl_6 \cdot 3H_2O$ was obtained from PCR, Inc. The phen and terp were from the G. F. Smith Chemical Company. Other materials including tetraethylammonium perchlorate (TEAP) from Eastman Kodak were reagent grade.

Analyses. Microanalyses were carried out by Atlantic Microlab, Inc. and Galbraith Laboratories, Inc.

Preparation of Complexes. $Ir(terp)_2^{3+}$ has not been previously reported. There is a literature preparation of $Ir(phen)_3^{3+}$.[15] However, given the enormous difficulty of isolating the pure complex, the simple literature preparation certainly does not yield a pure material. Both preparations here are analogous to the fusion reaction that was successfully used for the first preparation of $Ir(bpy)_3^{3+}$.[8]

$Ir(phen)_3^{3+}$. The preparation was a fusion reaction similar to that for the bpy complex. The purification necessary for obtaining chemically and spectroscopically pure material was complex and involved various solvent extractions, chromatography on several different systems, and recrystallizations. Details are given in the Supplementary Material. The final light yellow complex was isolated as a perchlorate. Anal. Calcd for $[Ir(C_{12}H_8N_2)_3](ClO_4)_3 \cdot (^3/_2)H_2O$: C, 40.86; H, 2.57; N, 7.94; Cl, 10.05. Found: C, 40.86; H, 2.66; N, 7.96; Cl, 10.14.

$Ir(terp)_2^{3+}$. The preparation was similar to that of $Ir(bpy)_3^{3+}$ and $Ir(phen)_3^{3+}$. The workup was equally arduous, and details are provided in the Supplementary Material.

The lemon yellow complex was isolated as the nitrate, trifluoroacetate, or perchlorate. Anal. Calcd for $[Ir(C_{15}H_{11}N_3)_2](NO_3)_3 \cdot 2H_2O$: C, 40.91; H, 2.98; N, 14.31. Found: C, 41.02; H, 3.00; N, 14.39; S, 0.00. Anal. Calcd for $[Ir(C_{15}H_{11}N_3)_2](CF_3CO_2)_3$: C, 43.34; H, 2.22; N, 8.42. Found: C, 41.94; H, 2.57 (1); N 8.89 (1); S, 0.00. Anal. Calcd for $[Ir(C_{15}H_{11}N_3)_2](ClO_4)_3 \cdot H_2O$: C, 36.95; H, 2.48; N, 8.62; Cl, 10.91. Found: C, 36.76; H, 2.43; N, 8.62; Cl, 10.75. Since all the complexes were spectroscopically identical and the perchlorate was obtained by metathesis of the trifluoroacetate, we conclude that trifluoroacetate interfered with the analysis.

Spectroscopic Measurements. All samples were handled in the dark, and light exposure was minimized to reduce sample decomposition. Monoexponential lifetime decay curves were obtained in all experiments so long as these precautions were followed.

Absorption spectra were measured on a Cary 17 spectrophotometer. Steady-state and decay time measurements used equipment and procedures described earlier.[11b] For emission spectra, the excitation slits were 16 nm and the emission slits 1 nm.

Typical emission measurements used 5–50 μM complex. For room-temperature measurements, the solvents were MeOH, MeCN, DMF, PrCN, and BuCN. For 77 K glass measurements we used 4:1 MeOH:H_2O, 4:5 PrCN:BuCN, 1:5 MeCN:BuCN, and 9:1 DMF:CH_2Cl_2.

Luminescence quantum yields, Φ's, were obtained by using a modified Parker–Rees method.[16,17] The yield of $Ir(phen)_3^{3+}$, measured against $Ru(bpy)_3^{3+}$ with an assumed yield of 0.042 in deaerated water,[18] was 8.6×10^{-4} in room-temperature deaerated MeOH. The $Ir(phen)_3^{3+}$ was used as the standard in all subsequent measurements because its emission spectrum more closely matches that of the systems studied.

Bimolecular quenching constants, k_q, were determined from Stern–Volmer quenching plots of the reciprocal lifetime, τ, versus quencher concentration:

$$1/\tau = k_r + k_{nr} + k_q[Q] \quad (1)$$

The radiative rate constants, k_r, and nonradiative rate constants, k_{nr}, were calculated by using

$$k_r = \frac{\Phi}{\Phi_{isc}\tau} \quad (2)$$

$$k_{nr} = (1 - \Phi)/\tau \quad (3)$$

where Φ_{isc} is the intersystem crossing efficiency, and τ is the lifetime under the same conditions. The k_r's and k_{nr}'s were calculated assuming $\Phi_{isc} = 1$.

NMR. ^1H NMR spectra were collected from methanol-d_4 solutions with a GE QE-300 Fourier Transform NMR spectrometer.

Data Fitting. All luminescence titration data were fit by using a simplex nonlinear least-squares method.[19]

(7) (a) Watts, R. J.; Brown, M. J.; Griffith, B. G.; Harrington, J. S. *J. Am. Chem. Soc.* **1975**, *97*, 6029. (b) Watts, R. J.; Griffith, B. G.; Harrington, J. S. *J. Am. Chem. Soc.* **1976**, *98*, 674. (b) DiBenedetto, J.; Watts, R. J.; Ford, P. C. *Inorg. Chem.* **1984**, *23*, 3039. (d) Cremers, T. L.; Crosby, G. A. *Chem. Phys. Lett.* **1980**, *73*, 541. (e) Watts, R. J.; Missimer, D. J. *J. Am. Chem. Soc.* **1978**, *100*, 5350. (f) Divisia, B.; Ford, P. C.; Watts, R. J. *J. Am. Chem. Soc.* **1980**, *102*, 7264.

(8) Flynn, C.; Demas, J. N. *J. Am. Chem. Soc.* **1974**, *96*, 1959.

(9) (a) Watts, R. J.; Crosby, G. A. *J. Am. Chem. Soc.* **1971**, *93*, 3184. (b) Watts, R. J.; Harrington, J. S.; Houten, J. Van *J. Am. Chem. Soc.* **1977**, *99*, 2179. (c) Watts, R. J. *Inorg. Chem.* **1981**, *20*, 2302.

(10) Demas, J. N.; Harris, E. W.; McBride, R. P. *J. Am. Chem. Soc.* **1977**, *99*, 3547.

(11) (a) Vogler, A.; Kunkely, H. *Inorg. Chim. Acta* **1980**, *43*, L265. (b) Ayala, N. P.; Demas, J. N.; DeGraff, B. A. *J. Am. Chem. Soc.* **1988**, *110*, 1523. (c) Ayala, N. P.; Demas, J. N.; DeGraff, B. A. *J. Phys. Chem.* **1989**, *93*, 4104. (d) Lever, A. B. P.; Seymour, P.; Auburn, P. R. *Inorg. Chim. Acta* **1988**, *145*, 43. (e) Nagle, J. K.; Brennan, B. A. *J. Am. Chem. Soc.* **1988**, *110*, 5931. (f) Palmer, C. E. A.; McMillin, D. R.; Kirmaier, C.; Holten, D. R. *Inorg. Chem.* **1987**, *26*, 3167. (g) McMillin, D. R.; Kirchoff, J. R.; Goodwin, K. V. *Coord. Chem. Rev.* **1985**, *64*, 83.

(12) Ohsawa, Y.; Sprouse, S.; King, K. A.; DeArmond, M. K.; Hanck, K. W.; Watts, R. J. *J. Phys. Chem.* **1987**, *91*, 1047.

(13) Grutsch, P. A.; Kutal, C. *J. Am. Chem. Soc.* **1986**, *108*, 3108.

(14) (a) DeGraff, B. A.; Demas, J. N. *J. Am. Chem. Soc.* **1980**, *102*, 6169. (b) Hauenstein, B., Jr.; Dressick, W. J.; Demas, J. N.; DeGraff, B. A. *J. Phys. Chem.* **1984**, *88*, 2418.

(15) Chiswell, B.; Livingstone, S. E. *Inorg. Nuclear Chem.* **1964**, *26*, 47.

(16) (a) Parker, C. A.; Rees, W. T. *Analyst (London)* **1960**, *85*, 587. (b) Parker, C. A. *Photoluminescence of Solutions*; Elsevier: New York, 1968.

(17) Demas, J. N.; Crosby, G. A. *J. Phys. Chem.* **1971**, *75*, 991.

(18) Van Houten, J.; Watts, R. J. *J. Am. Chem. Soc.* **1976**, *98*, 4853.

(19) (a) Daniels, R. W. *An Introduction to Numerical Methods and Optimization Techniques*; North Holland, Inc.: New York, 1978. (b) Demas, J. N. *Excited State Lifetime Measurements*; Academic Press: New York, 1983. (c) Demas, J. N.; Demas, S. E. *Interfacing and Scientific Computing on Personal Computers*; Allyn & Bacon: New York, 1990.

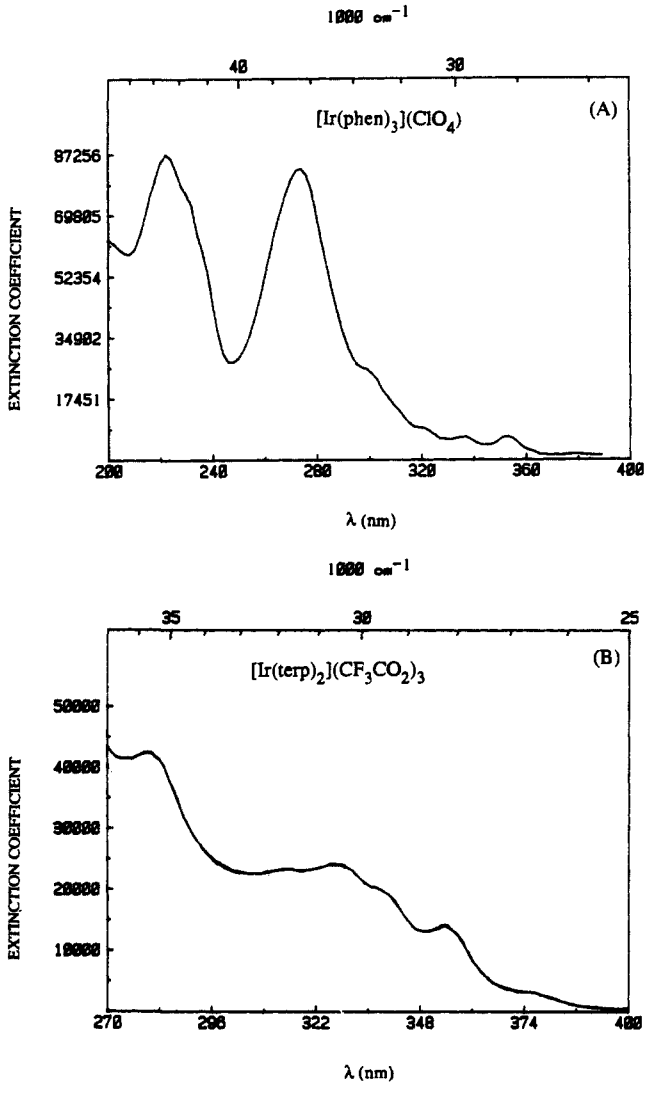

Figure 1. This figure shows (A) absorption spectrum $[Ir(phen)_3](ClO_4)_3$ in MeCN and (B) absorption spectrum $[Ir(terp)_2](CF_3CO_2)_3$ in MeCN.

Results

^1H NMR Spectra. The methanol-d_4 spectrum of $[Ir(phen)_3](ClO_4)_3 \cdot 2H_2O$ consists of four distinct resonances in the aromatic region, each having a relative integrated area of 1: δ 7.96 (br m), 8.16 (d), 8.47 (s), and 9.04 (d).

The spectrum of $[Ir(terp)_2](NO_3)_3 \cdot H_2O$ is slightly more complex with resonances at δ 7.53 (m), 7.85 (d), 8.25 (m), 8.83 (m), and 9.07 (d). The multiplet at 8.83 results from two overlapping resonances at 8.81 and 8.83 with relative integrated intensities of 2 and 1, respectively. All other aromatic resonances have relative integrated areas of 2.

Absorption Spectra. Figure 1 shows the absorption spectra of $Ir(phen)_3^{3+}$ and $Ir(terp)_2^{3+}$. In Figure 1A, the room-temperature absorption spectrum of $Ir(phen)_3^{3+}$ consists of three major peaks at 222 nm (ϵ = 94000 M^{-1} cm^{-1}), 273 nm (ϵ = 79000 M^{-1} cm^{-1}), and 303 nm (ϵ = 21 500 M^{-1} cm^{-1}) that are assigned to $\pi-\pi^*$ transitions by analogy with the protonated phen and $Rh(phen)_3^{3+}$ spectra.[20] Three peaks of lesser intensity for $Ir(phen)_3^{3+}$ occur at 322 nm (ϵ = 7440 M^{-1} cm^{-1}), 336 nm (ϵ = 5240 M^{-1} cm^{-1}), and 354 (ϵ = 5500 M^{-1} cm^{-1}). We assign these to $\pi-\pi^*$ transitions. Similar assignments have been made for $Ir(bipy)_3^{3+}$.[8]

The absorption spectrum of $Ir(terp)_2^{3+}$ in Figure 1B has peaks at 280 nm (ϵ = 42000 M^{-1} cm^{-1}), 315 nm (ϵ = 23000 M^{-1} cm^{-1}), 328 nm (ϵ = 25000 M^{-1} cm^{-1}), and 338 nm (ϵ = 20000 M^{-1} cm^{-1}).

(20) (a) Carstens, D. W. H. Ph.D. Dissertation, University of New Mexico, 1968. (b) Yamasaki, K. *Bull. Chem. Soc. Jpn.* **1937**, *12*, 390. (c) Sone, K.; Krumholz, P.; Stammreich, H. *J. Am. Chem. Soc.* **1955**, *77*, 777.

Table I. Radiative and Nonradiative Rate Constants

	τ_{obs} (μs)	Φ	k_r (s^{-1})	k_{nr} (s^{-1})
		$Ir(phen)_3^{3+}$		
		DMF		
no $HgCl_2$	1.72	0.0030	1700	5.8×10^5
limiting	4.3	0.010	2300	2.3×10^5
		MeCN		
no $HgCl_2$	3.5	0.0013	380	2.8×10^5
limiting	49.4	0.0106	214	2.0×10^4
		MeOH		
no $HgCl_2$	2.5	0.00086	340	4.0×10^5
limiting	0.4	0.00043	1100	2.5×10^6
		$Ir(terp)_2^{3+}$		
		MeCN		
no $HgCl_2$	0.070	4.6×10^{-5}	660	1.4×10^7
limiting	1.546	4.1×10^{-4}	260	6.5×10^5
		9:1 DMF:CH_2Cl_2		
no $HgCl_2$	0.228	1.84×10^{-4}	810	4.4×10^6
limiting	0.319	2.58×10^{-4}	810	3.1×10^6

These are assigned to $\pi-\pi^*$ transitions based on their similarity to the $\pi-\pi^*$ transition in $Zn(terp)^{2+}$ at 282, 305, 318, and 331 nm.[20] The peaks at 355 nm (ϵ = 13 800 M^{-1} cm^{-1}) and 378 nm (ϵ = 578) are probably predominantly d-π^* transitions; there are no corresponding peaks in the spectra of the protonated terp or $Zn(terp)^{2+}$.

Addition of millimolar amounts of $HgCl_2$ produced no discernible changes in the absorption spectra with either complex. Absorption by $HgCl_2$ may have masked changes below 270 nm.

Emission Spectra. The emission spectra of $Ir(phen)_3^{3+}$ and $Ir(terp)_2^{3+}$ are shown in Figure 2. The emission is clearly predominantly a $\pi-\pi^*$ phosphorescence.[8,20a] There is no overlap between the absorption and emission spectra. The emission's shapes are essentially insensitive to different solvents.

In Figure 2A, the 77 K emission spectrum of $Ir(phen)_3^{3+}$ (360-nm excitation) produces a rich family of peaks at 455, 485, 515, and 562 nm in 4:1 MeOH:H_2O. The pronounced 1300-cm^{-1} vibrational progression is typical of $\pi-\pi^*$ or CT emissions of complexes containing α-diimine ligands. The peak positions are unchanged in MeCN, DMF, and MeOH at room temperature. A 1.35 kK progression has been assigned to a breathing mode for phen ligands.[21]

In Figure 2B, the 77 K emission spectrum of $Ir(terp)_2^{3+}$ in 1:5 MeCN:BuCN matches very closely the relative peak shape of the $\pi-\pi^*$ phosphorescence of terp in $Zn(terp)^{2+}$ except for an approximately 1.2 kK red shift for the Ir complex.[20] Thus, the $Ir(terp)_2^{3+}$ emission is a metal perturbed intraligand $\pi-\pi^*$ phosphorescence.

In the 77 K glasses (4:1 MeOH:H_2O or 1:5 MeCN:BuCN), there are no significant changes in either the emission shapes or intensities on addition of $HgCl_2$; precise intensity comparisons are not possible in the glasses because of the difficulties of alignment. There are small lifetime changes (<6%) for $Ir(terp)_2^{3+}$ in 1:5 MeCN–BuCN at 77 K on added $HgCl_2$, but the effect is too small to unequivocally establish an interaction. There are no spectral shape changes in room-temperature solutions on adding $HgCl_2$ (e.g., Figure 2C), although the emission intensities can either increase greatly or decrease depending on the solvent. Thus, there is no compelling evidence for formation of new ground-state species in the presence of $HgCl_2$.

Quantum Yields and Lifetimes. Quantum yields were calculated by using the relative emission heights as $HgCl_2$ was added since the shapes of the emission spectra are unchanged. Room-temperature emission quantum yields are shown in Table I. For the cases studied, $HgCl_2$ increases the yields for the Ir(III)–α-diimine complexes in MeCN, DMF, and 9:1 DMF:CH_2Cl_2 and decreases the yields in MeOH, but the kinetics are not Stern–Volmer (vide

(21) Caspar, J. V.; Meyer, T. J. *J. Am. Chem. Soc.* **1983**, *105*, 5583.

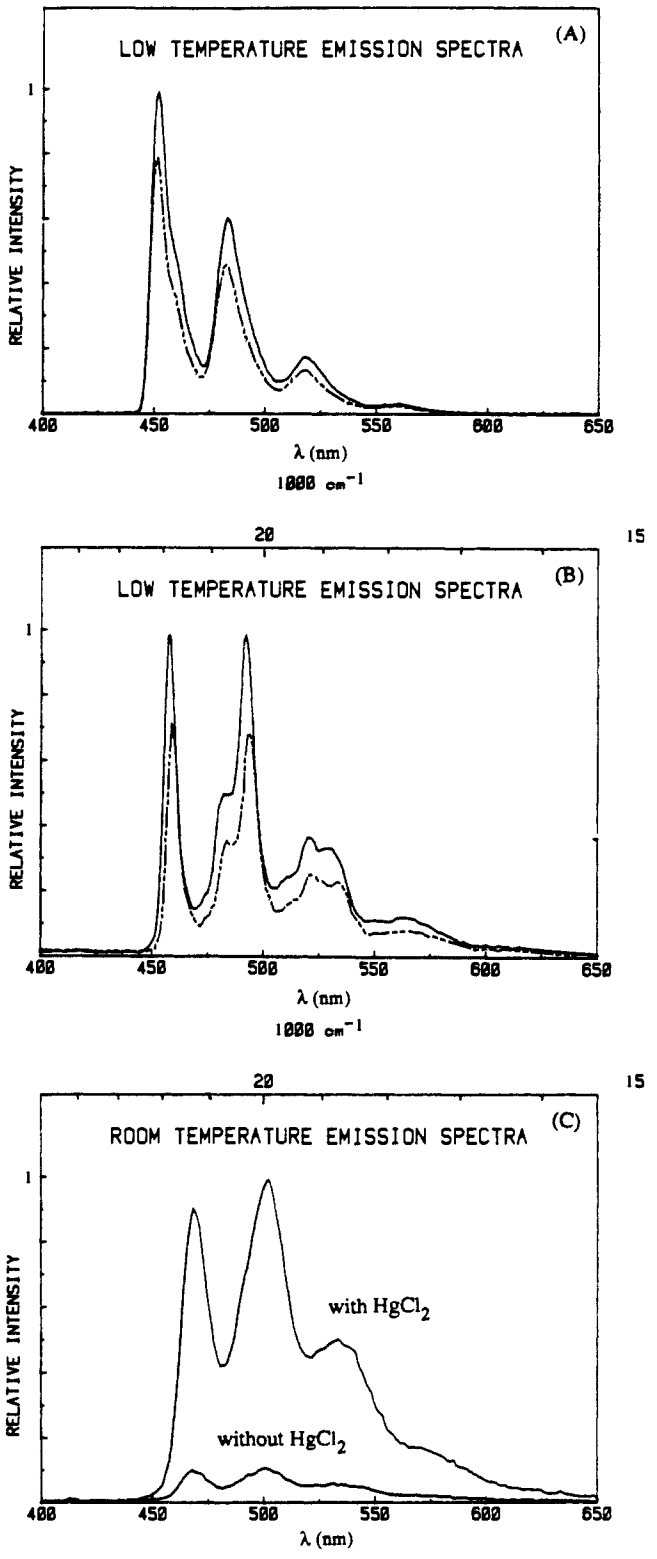

Figure 2. This figure shows (A) low-temperature emission spectrum $[Ir(phen)_3](ClO_4)_3$ in 4:1 MeOH:H_2O, (B) low-temperature emission spectrum $[Ir(terp)_2](CF_3CO_2)_3$ in 1:5 MeCN:BuCN, and (C) room-temperature emission spectrum $[Ir(terp)_2](CF_3CO_2)_3$ in MeCN. The dashed lines are with 4.8 mM $HgCl_2$.

infra). For comparison, $Ir(phen)_2Cl_2^+$ and $Ir(bpy)_2Cl_2^+$ have unquenched quantum yields in deaerated methanol of 6.4×10^{-4} and 9.2×10^{-4}.

$HgCl_2$ in MeCN quenched $Ir(phen)_2Cl_2^+$ and $Ir(phen)_2Br_2^+$ by normal diffusional quenching as shown by linear lifetime Stern–Volmer plots. Stern–Volmer quenching constants, K_{sv}, of 50 ± 10 M^{-1} for $Ir(phen)_2Cl_2^+$ and 260 ± 50 M^{-1} for $Ir(phen)_2Br_2^+$, were obtained. The bimolecular quenching constants were 1.8×10^8 M^{-1} s^{-1} for $Ir(phen)_2Cl_2^+$ and 9.5×10^8 M^{-1} s^{-1} for $Ir(phen)_2Br_2^+$.

For both $Ir(phen)_3^{3+}$ and $Ir(terp)_2^{3+}$ addition of $HgCl_2$ dramatically affects the emission lifetimes and intensity. Figure 3 shows typical lifetime titration curves. At very high concentration (>50 mM) in MeCN, the lifetimes of $Ir(phen)_3^{3+}$ did decrease slowly but generally never fell below the value in the absence of $HgCl_2$. In contrast, for $Ir(terp)_2^{3+}$ in deaerated BuCN, 1:5 MeCN:BuCN, and PrCN, the lifetimes increased sharply to a maximum between 1 and 2 mM $HgCl_2$ and then decreased rapidly to a value below the original lifetime. We have not studied these longer chain solvent systems further.

For systems containing $HgCl_2$, limiting quantum yields and lifetimes were obtained from samples containing at least 10 mM $HgCl_2$. Where necessary, corrections were applied for any non-complexed iridium species present.

Surprisingly, addition of an inert ClO_4^- salt radically affects the lifetime and the impact of $HgCl_2$. In the presence of large amounts of perchlorate, $HgCl_2$ has a minimal effect on the excited-state lifetimes (compare Figure 4A and B with Figure 3). This arises in part from the large variation in excited-state lifetime with $[ClO_4^-]$ in the absence of $HgCl_2$ (Figure 4C for MeCN). $Ir(phen)_3^{3+}$ is similar, and data are shown in the original thesis.[22]

Addition of Cl^- as Me_4NCl, Bu_4NCl, or LiCl to deoxygenated MeCN solutions of $Ir(phen)_3^{3+}$ containing $HgCl_2$ decreased lifetimes without emission shape changes. The concentration of Cl^- exceeded the amount of $HgCl_2$ present.

Stern–Volmer constants for O_2 quenching, $K_{sv}(O_2)$, and bimolecular quenching constants are listed in Table II. For the $HgCl_2$ titrations, the $k_q(O_2)$'s decrease slightly with increasing $[HgCl_2]$.[22]

Discussion

Structure. In view of the past difficulty of establishing the structures of Ir(III)–α-diimine complexes, we first turn to the structure elucidation. Microanalysis coupled with ^1H NMR unequivocally proves that the complexes are $Ir(phen)_3^{3+}$ and $Ir(terp)_2^{3+}$.

$Ir(phen)_3^{3+}$ should have four magnetically distinct protons; these are observed in the spectrum in equal ratio. Thus, the three phen ligands are N-coordinated. The singlet at δ 8.47 is assigned to the H5 proton, while the multiplet at 7.96 corresponds to H3, which is split by both the H2 and H4 protons. The doublet at δ 9.04 corresponds to H4, which is split by H3. The H2 doublet usually occurs at low field in monochelated phenanthroline complexes, but it is shifted to higher field (δ 8.16) in $Ir(phen)_3^{3+}$. Models show that this proton is located near the face of an adjacent aromatic ring. A similar effect has been observed for the H6 proton of $Ru(bpy)_3^{2+}$ where the shift was explained by a diamagnetic anisotropic effect of the adjacent bipyridine ligand.[23,24] We find that the ^1H NMR spectrum of $Ru(phen)_3^{2+}$ in D_2O shows the same pattern of resonances as $Ir(phen)_3^{3+}$.

The $Ir(terp)_2^{3+}$ spectrum is consistent with planar terp bound only through the N atoms. The two terp ligands are chemically indistinguishable, and a 2-fold axis passes through the H4′ protons. This structure has six types of proton environments. The spectrum shows four distinct resonances and a multiplet that must arise from two overlapping resonances. Assignments may be made by comparison with the published spectra of $Os(terp)_2Cl_2$ in ethanol and $Ru(terp)_2I_2$ in DMSO-d_6.[24] The multiplet at δ 7.53 corresponds to H5, and the H6 proton appears as a doublet at 7.85. As in the case of the H2 of $Ir(phen)_3^{3+}$, this proton is located near the face of the adjacent ligand and is shifted upfield from the free ligand. The resonance at 8.25 arises from H4, and the low field doublet is assigned as H3′. The multiplet at 8.83 results from overlap of the H4′ multiplet at 8.85 and the H3 doublet at 8.81. The integration is consistent with this conclusion, the H4′ proton

(22) Ayala, N. P. Ph.D. Thesis, University of Virginia, 1988.
(23) Bryant, M.; Fergusson, J. E. *Austr. J. Chem.* **1971**, *24*, 441–444.
(24) Lytle, F. E.; Petrosky, L. M.; Carlson, L. R. *Anal. Chim. Acta* **1971**, *57*, 239–247.

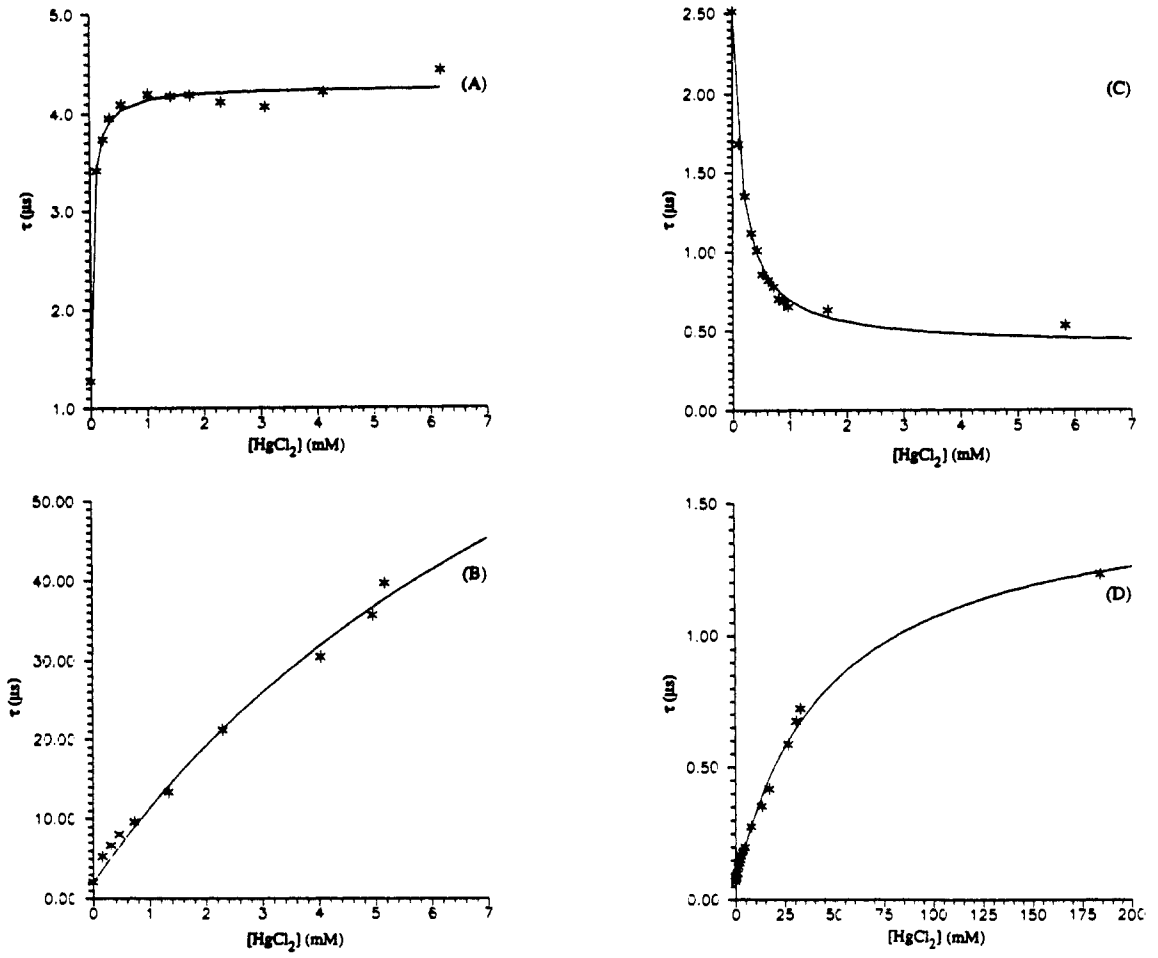

Figure 3. This figure shows (A) lifetime titration $Ir(phen)_3^{3+}$ with $HgCl_2$ in DMF, (B) lifetime titration $Ir(phen)_3^{3+}$ with $HgCl_2$ in MeCN, (C) lifetime titration $Ir(phen)_3^{3+}$ with $HgCl_2$ in MeOH, and (D) lifetime titration $Ir(terp)_2^{3+}$ with $HgCl_2$ in MeCN. In all cases solid curves are simplex fit to lifetime data (*) by using eq 7. Parameters for the best fit are in Table III.

has been observed to shift downfield relative to the other protons when the metal is changed from Os to Ru.[24] This shift is explained in terms of decreasing effective charge density at the three terp N atoms. It is therefore not surprising that the H4′ proton of $Ir(terp)_2^{3+}$ is shifted even more downfield resulting in overlap with H3 because of the tripositive Ir center.

Spectra. In the absorption and emission spectra of Ir(III)–α-diimine complexes, there are metal-to-ligand charge-transfer (MLCT) transitions (d–π*) and ligand localized transitions (π–π*).[7-9] The peaks in the absorption spectra above 300 nm for $Ir(phen)_3^{3+}$ and $Ir(terp)_2^{3+}$ are clearly predominantly ligand-localized π–π* transitions, with possibly a small CT contribution. Ligand photosubstitution provides evidence for low-lying ligand field (d–d*) transitions in $IrL_2Cl_2^+$.[25] The degree of d–π*/π–π* mixing depends strongly on the α-diimine and the coordinated halide.

The emission of $Ir(phen)_2Cl_2^+$ was assigned to a predominantly d–π* transition with some π–π* character.[7d] As the solvent polarity increased, the lower level ^{3}d–π* state is raised in energy closer to the ^{3}π–π* state; the decreased energy gap increases mixing of the ^{3}π–π* state into the emitting ^{3}d–π* state, which increases the ligand character of the emission of $Ir(phen)_2Cl_2^+$ in polar solvents.[9c]

Similar to our earlier work with $Ir(bpy)_3^{3+}$,[8] we assign the emission of $Ir(phen)_3^{3+}$ and $Ir(terp)_2^{3+}$ to predominantly ligand-localized phosphorescences. This is based on both the lifetimes and the emission spectra.

The radiative lifetimes ($\tau_r = 1/k_r$) for $Ir(phen)_3^{3+}$ and $Ir(terp)_2^{3+}$ in the absence of $HgCl_2$ are 600–3000 μs depending on solvent. These radiative lifetimes are much too long to be predominantly MLCT emissions. Pure ligand emissions would be longer still (i.e., >10 ms); thus, the dominant contribution to the allowedness of the ^{3}π–π* emission is probably mixing of more allowed MLCT states. The variations of τ_r with solvent are no doubt due to variations of the MLCT state energy with concomitant changes in the MLCT/π–π* mixing efficiency. For example, in Table II, the much longer room-temperature τ in polar solvents (70 μs in H_2O for $Ir(phen)_3^{3+}$ compared to 3.7 μs in MeCN) is explained by an increase in energy of the d–π* level relative to the π–π* level as the polarity of the solvent increases. Less contribution of the shorter lived d–π* state with the predominantly longer lived π–π* level increases the lifetime of $*Ir(phen)_3^{3+}$ in

Table II. Room-Temperature Lifetimes and Oxygen-Quenching Constants

	τ_{N2} (μs)	τ_{air} (μs)	$K_{sv}(O_2)$ (M^{-1})	$k_q(O_2)$ (M^{-1} s^{-1})
	$[Ir(phen)_2Cl_2]Cl$			
MeCN	0.32	0.24	210	6.4×10^8
	$[Ir(phen)_2Br_2]Br$			
MeCN	0.27	0.23	110	4.0×10^8
	$[Ir(phen)_3](ClO_4)_3$			
MeCN	3.7	1.9	590	1.6×10^8
0.16 M TEAP/MeCN	4.6	2.1	750	1.6×10^8
0.7 M $LiClO_4$/MeCN	10.41	2.19	2300	2.2×10^8
1:1 H_2O:EtOH	30.0	14.0	1000	3.3×10^8
H_2O	70.0	8.7	29000	4.2×10^8
4:1 MeOH:H_2O	1013 (77 K)			
	$[Ir(terp)_2](O_2CCF_3)_3$			
9:1 DMF:CH_2Cl_2	0.227	0.200	136	6.0×10^8
MeCN	0.070			
0.126 M TEAP/MeCN	0.634	0.527	126	2.0×10^8
0.7 M $LiClO_4$/MeCN	1.074	0.818	194	1.8×10^8
5:1 BuCN:MeCN	26.4 (77 K)			

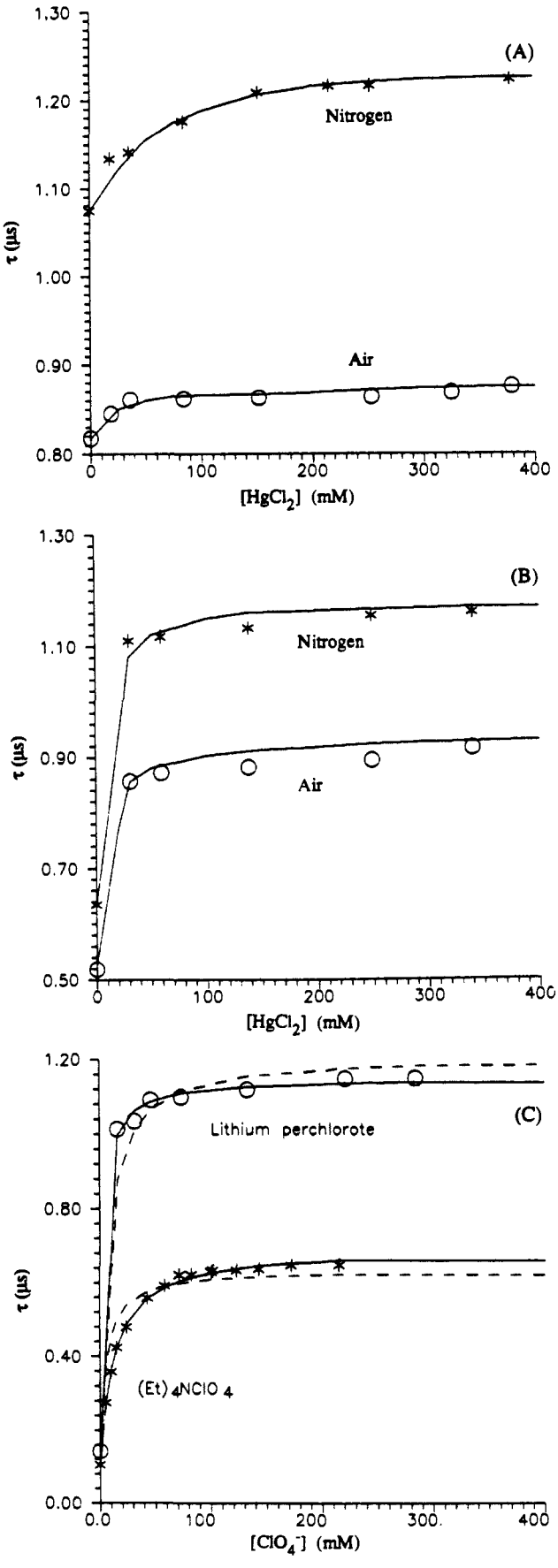

Figure 4. This figure shows lifetime titration of $Ir(terp)_2^{3+}$ with $HgCl_2$ in (A) 0.664 M $LiClO_4$/MeCN and (B) 0.126 M TEAP/MeCN. *'s are deoxygenated and o's are air saturated. Solid lines are the best fits using eq 10 and the parameters of Table IV. Part (C) shows ClO_4^- titrations of $Ir(terp)_2^{3+}$ in deoxygenated MeCN using $LiClO_4$ (o) and TEAP (*). Dashed curves are the best fits using only a 1:1 ion pair.

polar solvents. This is similar to the solvent dependencies reported earlier by Watts.[9c]

The emission spectra also support a $\pi-\pi^*$ phosphorescence assignment for $Ir(phen)_3^{3+}$ and $Ir(terp)_2^{3+}$. The phosphorescence of free or coordinated phen (E_{00} = 22.2 kcm^{-1}) matches closely the emission of the $Ir(phen)_3^{3+}$ (E_{00} = 22.5 kcm^{-1}) but is significantly different from the d-π^* emission of $Ir(phen)_2Cl_2$ (E_{00} = 21.1 kcm^{-1}). The greater similarity of the $Ir(phen)_3^{3+}$ emission to a pure ligand phosphorescence coupled with its long τ_r establishes that it is predominantly a ligand localized $\pi-\pi^*$ phosphorescence. Similarly, the emission spectrum of $Ir(terp)_2^{3+}$ closely resembles in structure the ligand phosphorescence of $Zn(terp)^{2+}$.[20a]

$HgCl_2$ Effects. We next consider the mechanism for emission enhancement in the presence of $HgCl_2$. This could arise from changes in the intersystem crossing yields or in the radiative and nonradiative rate constants. The intersystem crossing yield, Φ_{isc}, is given by

$$\Phi_{isc} = k_{isc}/(k_r + k_{nr} + k_{isc}) \quad (4)$$

where k_{isc} is the intersystem crossing rate constant. For a large number of Ru(II)- and Os(II)-α-diimine complexes examined in water and methanol at room temperature, Φ_{isc} is 1.[26] $Ir(bpy)_3^{3+}$ and $Ir(phen)_3^{3+}$ also have Φ_{isc} of approximately unity.[10] In the absence of any other evidence, we assume that Φ_{isc} for $Ir(terp)_2^{3+}$ is also 1. Thus, it seems unlikely that the changes in yield with $[HgCl_2]$ can be ascribed to changes in Φ_{isc}.

The observed emission quantum yield is

$$\Phi_{obs} = \Phi_{isc}k_r/(k_r + k_{nr} + k_q[Q]) \quad (5)$$

At least in DMF and MeCN, the Φ_{obs}'s increase with *quencher* concentration. For example, Φ_{obs} increases by a factor of 9 and τ by a factor of 22 for $Ir(terp)_2^{3+}$ in MeCN with $HgCl_2$. Thus, in these cases a dynamic quenching model is not applicable. As shown by Table I, the major cause (ignoring bimolecular quenching) of the increase in Φ_{obs} in DMF and MeCN arises from a decreased k_{nr}. In MeOH, $HgCl_2$ affects both k_r and k_{nr}, but the behavior cannot be fit by bimolecular quenching.

Excited-State Complex Model. Since the changes in τ and Φ_{obs} on addition of $HgCl_2$ cannot be accounted for by collisional quenching, we must invoke a model including formation of stable Ir(III)-$HgCl_2$ excited-state species with different emissive properties. The following model fits our data:

$$^*D + HgCl_2 \underset{}{\overset{K_{ex}}{\rightleftharpoons}} {}^*DHgCl_2$$
$$\downarrow 1/\tau_o \qquad \downarrow 1/\tau_{ex}$$
$$D \qquad D + HgCl_2$$

K_{ex} is the association constant for formation of the excited-state complex. The fractions of $^*D(f_0)$ and $^*DHgCl_2(f_{ex})$ are given by

$$f_0 = 1/(1 + K_{ex}[HgCl_2]) \quad (6a)$$

$$f_{ex} = K_{ex}[HgCl_2]/(1 + K_{ex}[HgCl_2]) \quad (6b)$$

The lifetime as a function of $HgCl_2$ concentration is given by

$$1/\tau_{obs} = f_0/\tau_0 + f_{ex}/\tau_{ex} \quad (7)$$

where τ_0 and τ_{ex} are the lifetimes of $^*D$ and $^*DHgCl_2$, respectively. For τ_{ex} the limiting τ at infinite $[HgCl_2]$ was used.

Equation 7 successfully explains the changes in τ's for the $Ir(phen)_3^{3+}$ and $Ir(terp)_2^{3+}$ as shown in Figure 3. The solid lines are the best fits with the K_{ex}'s and τ_{ex}'s in Table III. This model works even for MeOH (Figure 3C), where the lifetime decreases but gives a plateau that cannot be accounted for by Stern-Volmer kinetics.

We suggest that the driving force for the association arises from the well-known affinity of $HgCl_2$ for aromatic hydrocarbons; this is a Lewis acid-base charge-transfer complex in which the aromatic molecule serves as the donor, while the $HgCl_2$ is the acceptor.[27] In the absence of extra electrolytes, the K_{ex}'s are greater

Table III. Exciplex Parameters for Ir(III)–α-Diimine Complexes with $HgCl_2$

	τ_{obs} (μs)	K_{ex} (M^{-1})	τ_{ex} (μs)	$K_{SVex}(O_2)$ (M^{-1})	$k_{qex}(O_2) \times 10^{-8}$ (M^{-1} s^{-1})
		$Ir(phen)_6^{3+}$			
DMF	1.7	67000	4.3		
MeCN/no salt	3.5	4900	49.4		
MeCN/0.16 M TEAP	4.6	480	10.8	2300	2.1
MeCN/0.7 M $LiClO_4$	10.4	19	12.2	2550	2.1
MeOH	2.5	960	0.4		
		$Ir(terp)_2^{3+}$			
MeCN/no salt	0.07	460	1.55		
MeCN/0.126 M TEAP	0.64	310	1.18	168	1.4
MeCN/0.7 M $LiClO_4$	1.07	28	1.24	252	2.0
9:1 DMF/CH_2Cl_2	0.23	150	0.32	117	3.7

for $Ir(phen)_3^{3+}$ than for $Ir(terp)_2^{3+}$, which is commensurate with the greater aromatic character of $Ir(phen)_3^{3+}$ versus $Ir(terp)_2^{3+}$.

Addition of $LiClO_4$ or TEAP greatly decreases the K_{ex}'s and at high [ClO_4^-] there is a leveling effect. We suggest formation of ClO_4^- ion pairs that hinder complex formation. Both steric effects and perturbation of the solvent environment could be involved.

Changes of Φ's and τ's on addition of $HgCl_2$ depend on the solvent and the complex. These variations arise from changes in k_r and k_{nr}. We turn now to the origin of these changes and the information that can be extracted. Examination of k_r's on addition of $HgCl_2$ provides insight into changes in the orbital and spin parentage of the emitting level on association. Invariance of k_r shows that the spin and orbital parentage of the emission are unaffected. Increases in k_r indicate an increased allowedness or more singlet character of the emission, while a decreased k_r reveals a reduction in the singlet character of the emitting level.

In spite of the large effects of $HgCl_2$ association on the τ's and Φ's, there is no change in the shape or energies of the emission spectra. Thus, $HgCl_2$ cannot radically change the overall $\pi-\pi^*$ character of the emitting state.

The dominant source of changes in Φ and τ is variations in k_{nr}. The observed decay rates track the changes in k_{nr}. Except for MeOH, the k_{nr}'s decrease on addition of $HgCl_2$. We suggest that the decreased k_{nr}'s are due to mercury-mediated solvent perturbations of state energies and a concomitant mixing of the different excited states.

However, in MeOH, $HgCl_2$ increases k_{nr}. MeOH is the only hydroxylic solvent studied, and OH vibrations are particularly good deactivators of excited states.[28,29] In methanol, $HgCl_2$ is solvated with two MeOH's through Hg–O bonds and hydrogen bonded with two MeOH's through the chlorides to form $[HgCl_2(MeOH)_2](MeOH)_2$. Thus, on association with the Ir(III) complex, the OH's in $^*DHgCl_2(MeOH)_2(MeOH)_2$ are directly attached to the iridium complex and provide a more efficient deactivation pathway than bulk OH's. Such a deactivation mechanism cannot be present in MeCN or DMF.

The variations in k_r present a complex picture. Possible factors that can affect k_r are a heavy atom enhanced k_r from the $HgCl_2$, variations in CT state energies with solvent perturbations (which changes the mixing of the more allowed CT states into the emitting $\pi-\pi^*$ level), or specific solvent interactions with the excited Hg complex.

A heavy atom effect should increase the singlet character of the emitting state and increase k_r. However, this is probably not a significant factor. If a simple heavy atom effect were operative, all the k_r's should increase independent of solvent. The k_r's show a complex relationship with complex and solvent. Only $Ir(phen)_3^{3+}$ in methanol has an increased k_r on $HgCl_2$ association. The absence of a simple heavy atom perturbation by Hg is not surprising. Mercury with a Z of 80 should have little effect on a complex, which already has an Ir with a Z of 77.

We suggest an alternative explanation for the complex variations in the k_r's. Clearly solvent is important. The state energies of CT levels are sensitive to solvent variations,[21] while the ligand $\pi-\pi^*$ levels are essentially insensitive. The k_r's for CT emission are much greater than those of $\pi-\pi^*$ phosphorescences. Since CT energies change with solvent variations, the degree of mixing of the more allowed CT states into the emitting $\pi-\pi^*$ level will be altered with solvent and association with $HgCl_2$. The more CT character, the larger k_r. The complexity of such interactions is increased since the solvent shifts of CT state energies depend on symmetry. $IrL_2Cl_2^+$ has different solvent effects than trigonal OsL_3^{2+} and RuL_3^{2+}.

Exciplex versus Ground-State Complex. We address the question of whether the new excited-state species is a true exciplex. A true exciplex has a dissociative ground state. Dissociative ground states should, however, yield a red shift in the emission spectrum; this emission shift arises from loss of energy on formation of the exciplex and emission to the more energetic dissociative form of the ground state. We see no detectible shift even though a Förster cycle predicts easily detectible shifts. On the other hand, there is no absorption evidence to indicate formation of a ground-state complex. Our assumption is that the excited-state complex does have a ground-state counterpart and is, thus, not a true exciplex. However, the new ground state species is spectrally too similar to the parent iridium complex to be detected.

The failure to detect absorption spectral changes is not surprising. As has been observed for the interactions of $HgCl_2$ with aromatic hydrocarbons such as benzene, the spectral perturbations can be minimal despite clear evidence for association.[27] The absence of emission change may reflect either the small perturbation of the state properties on binding or arise from binding of the $HgCl_2$ at a phen or terp not directly involved in the emission. Localization of $^3(\pi-\pi^*)$ excited states is well-known in bpy and phen complexes.[30]

Oxygen-Quenching Effects. Quenching by O_2 of the $\pi-\pi^*$ triplet states of $IrL_{2,3}^{3+}$–α-diimine complexes has been shown to produce singlet O_2 with a near unit efficiency and high quenching rates somewhat below the diffusion-controlled limit.[10] As shown in Table II, the oxygen bimolecular quenching constants in the absence of $HgCl_2$ range from 1.6×10^8 to 6×10^8 M^{-1} s^{-1}. To treat simultaneous oxygen quenching and excited-state complex formation, eq 7 is modified to

$$1/\tau_{obs} = (1 + K_{sv}[O_2])\frac{f_0}{\tau_0} + (1 + K_{SVex}[O_2])\frac{f_{ex}}{\tau_{ex}} \quad (8)$$

where K_{SV} is the Stern–Volmer constant for O_2 quenching in the absence of $HgCl_2$, K_{SVex} is the limiting Stern–Volmer constant for O_2 quenching of the complex, f_0 and f_{ex} are given by eq 6, and [O_2] is the solution oxygen concentration. For deoxygenated solutions, eq 8 reduces to eq 7. The simplex best fit parameters for the N_2 and air-saturated lifetime data are listed in Tables II and III. Comparison of k_q and k_{qex} shows that the excited-state complex has, within experimental error, the same oxygen-quenching constants as the unassociated complex.

The failure to see any shielding of the $HgCl_2$ association complex from O_2 may again be a consequence of localized excitation. If the $HgCl_2$ is on a ligand different from the emitting one, then one would expect no changes in the quenching rate constant; no changes were observed. This effect is opposite to what we see in

(25) Ballardini, R.; Varani, G.; Moggi, L.; Balzani, B.; Olson, K. R.; Scandola, F.; Hoffman, M. Z. *J. Am. Chem. Soc.* **1975**, *97*, 728.
(26) (a) Demas, J. N.; Taylor, D. G. *Inorg. Chem.* **1979**, *18*, 3177. (b) Taylor, D. G.; Demas, J. N. *J. Chem. Phys.* **1979**, *71*, 1032.
(27) (a) Eliezer, I. J. *Chem. Phys.* **1965**, *42*, 3625. (b) Eliezer, I.; Anivur, P. J. *Chem. Phys.* **1971**, *55*, 2300. (c) Vezzos, I. M.; Peyronal, G.; Zanoli, A. F. *Inorg. Chim. Acta* **1974**, *8*, 229. (d) Mulliken, R. S.; Pearson, W. B. *Molecular Complexes*; Wiley and Son: New York, 1969.
(28) (a) Kropp, J. L.; Windsor, M. W. *J. Phys. Chem.* **1967**, *71*, 477. (b) Horrocks, W. DeW., Jr.; Sudnick, D. R. *Acc. Chem. Res.* **1981**, *14*, 384.
(29) Hauenstein, B. L., Jr.; Dressick, W. J.; Buell, S. L.; Demas, J. N.; DeGraff, B. A. *J. Am. Chem. Soc.* **1983**, *105*, 4251.
(30) Halper, W.; DeArmond, M. K. *J. Lumin.* **1972**, *5*, 225.

Table IV. Ion Pair Constants for ClO_4^- in MeCN

	$LiClO_4$	$(CH_3)_4NClO_4$
	$Ir(phen)_3^{3+}$	
log K_1	3.14	3.14
log K_2	0.65	0.65
τ_0 (μs)	4.0	2.6
τ_1 (μs)	7.65	3.74
τ_2 (μs)	12.88	6.97
	$Ir(terp)_2^{3+}$	
log K_1	3.8	3.8
log K_2	2.7	2.7
τ_0 (μs)	1.12	0.26
τ_1 (μs)	0.46	0.10
τ_2 (μs)	1.15	0.69

the RuL_3^{2+}–cyclodextrin systems where the cyclodextrin binds at the site of localized excitation and disproportionately decreases oxygen quenching.[31]

Effect of Inert Anions on Excited-State Complex Formation. There are three possible ion-pairing equilibria. We show these below for perchlorate:

$$IrL_n^{3+} + ClO_4^- \leftarrow K_1 \rightarrow IrL_n^{3+}|(ClO_4^-) \quad (9a)$$

$$IrL_n^{3+}|(ClO_4^-) + ClO_4^- \leftarrow K_2 \rightarrow IrL_n^{3+}|(ClO_4^-)_2 \quad (9b)$$

$$IrL_n^{3+}|(ClO_4^-)_2 + ClO_4^- \leftarrow K_3 \rightarrow IrL_n^{3+}|(ClO_4^-)_3 \quad (9c)$$

where n is 2 or 3 for the terp or phen complexes, respectively.

The three stability constants for ClO_4^- ion pair formation in water with $Ir(phen)_3^{3+}$ were found by solubility measurements to be log K_1 = 1.9, log K_2 = 1.1, log K_3 = 0.9.[32] In H_2O, $K_1 > K_2 > K_3$ due to the decreased electrostatic charges of the higher ion pairs.

Compared to the M(II)–α-diimine (M = Fe, Ru, Ni) complexes,[33] ion-pairing constants are larger for M(III)–α-diimine complexes (M = Ir, Cr) due to the larger 3+ charge.[34] Ion-pairing constants are expected to be greater in MeCN compared to water based on the Eigen–Fuoss equation.[35] To investigate the validity of these expectations, simplex fitting of the lifetime data as a function of concentration of ClO_4^- was performed by using several ion-pairing models.

Initially, we tried a simple model with only a single equilibrium for the formation of a 1:1 ion pair. As shown by the dashed line in Figure 4C, a single ion pair equilibrium model fails.

Next a model was considered with equilibria for the formation of 1:1 and 1:2 ion pairs. The lifetime can be calculated with

$$1/\tau_{obs} = f_0/\tau_0 + f_1/\tau_1 + f_2/\tau_2 \quad (10)$$

where f_0, f_1, and f_2 are given by eq 11 and $\tau_{1,2}$ are the lifetimes for the 1:1 and 1:2 ion pairs.

$$f_0 = \frac{1}{(1 + K_1[ClO_4^-] + K_1K_2[ClO_4^-]^2)} \quad (11a)$$

$$f_1 = K_1[ClO_4^-]f_0 \quad (11b)$$

$$f_2 = K_1K_2[ClO_4^-]^2f_0 \quad (11c)$$

Global simplex fitting of eq 10 to the τ data versus [$LiClO_4$] and [TEAP] was performed by using the same equilibrium constants, K_1 and K_2, and different lifetimes, $\tau_1(LiClO_4)$, $\tau_2(LiClO_4)$, $\tau_1(TEAP)$, and $\tau_2(TEAP)$, for the ion pairs in $LiClO_4$ and TEAP solution. The same equilibrium constants, K_1 and K_2, were used in the global simplex fitting of eq 10 to the lifetime data for both $LiClO_4$ and TEAP titrations, since the cations are not expected to influence the magnitude of ClO_4^- ion pairing. This model successfully fits the lifetime data in Figure 4C for $Ir(terp)_2^{3+}$ and also for $Ir(phen)_3^{3+}$. The best fit K's are given in Table IV.

Fits of the τ data using a three-equilibria ion-pairing model did not produce significantly better fits, although the K's decreased as expected: $K_1 > K_2 > K_3$. Since a three-equilibrium model must be more nearly correct based on the charge ratios, our results suggest that the three-to-one ion pair must have luminescence properties that differ only slightly from the two-to-one ion pair. Our K_2's must represent some average of the actual K_2 and K_3.

As predicted, the K's for $Ir(phen)_3^{3+}$ increase on going from water[32] to MeCN. The K_2's are smaller than K_1's because of decreased electrostatic attraction.

Chloride Effects. One possible mechanism for interaction of $HgCl_2$ with the Ir(III) cationic species would be for the establishment of an equilibrium of Hg^{2+} species.

$$HgCl_2 + Cl^- \leftarrow K_1 \rightarrow HgCl_3^- + Cl^- \leftarrow K_2 \rightarrow HgCl_4^{2-} \quad (12)$$

Ion pairing with $HgCl_3^-$ and $HgCl_4^{2-}$ could produce new luminescent species. To test this hypothesis, we added additional Cl^- with the $HgCl_2$; this should increase the concentrations of Hg(II) anionics and enhance the effects seen with only $HgCl_2$.

For $Ir(phen)_3^{3+}$ in MeCN, titrations were done with $HgCl_2$–LiCl or $HgCl_2$–(*t*-BuN)$_4$Cl with a Hg to LiCl or (*t*-BuN)$_4$Cl ratio of about 1:2. In the (*t*-BuN)$_4$Cl case only quenching was observed, while with LiCl a small increase in τ was found (2–3.6 μs at 0.2 mM Hg^{2+}). Thus, the large effect of $HgCl_2$ observed in the absence of extra Cl^- is greatly reduced or eliminated when excess Cl^- is added, even at very low concentrations. We conclude that the dominant species present and responsible for the enhanced luminescence in MeCN systems are $IrL_{2,3}^{3+}$–$HgCl_2$ complexes.

Conclusions

One of the important areas of research for transition-metal complexes is the development of luminescent environmentally sensitive molecules.[36] In the past this work has focused on complexes with predominantly MLCT emissions. $Ir(phen)_3^{2+}$ and $Ir(terp)_2^{3+}$ with π–π^* emissions show exceptionally large sensitivities to subtle environmental changes. Our work shows that a novel excited-state complex forms between $Ir(phen)_3^{3+}$ and $Ir(terp)_2^{3+}$ with $HgCl_2$. The lifetimes and intensities can increase by about an order of magnitude. Solvent changes can radically alter the observed interactions. We suggest that this effect has its origins in the well-known interaction of $HgCl_2$ with extended π systems. These results suggest that these complexes may prove to be valuable model systems for new environmental probes.

Acknowledgment. We gratefully acknowledge the support of the National Science Foundation (Grant CHE 86-00012 and 88-17809). We gratefully acknowledge Mark G. Robertson for preliminary titrations.

Supplementary Material Available: Details of the synthesis of $Ir(phen)_3^{3+}$ and $Ir(terp)_2^{3+}$ (3 pages). Ordering information is given on any current masthead page.

(31) Cline III, J. I.; Dressick, W. J.; Demas, J. N.; DeGraff, B. A. *J. Phys. Chem.* **1985**, *84*, 94.

(32) (a) Pyartman, A. K.; Sof'in, M. V.; Mironov, V. E. *Russ. J. Inorg. Chem.* **1984**, *29*, 915. (b) Pyartman, A. K.; Sof'in, M. V.; Mironov, V. E. *Russ. J. Inorg. Chem.* **1983**, *28*, 1153. (c) Bizunok, M. B.; Pyartman, A. K.; Belovsov, E. A. *Russ. J. Inorg. Chem.* **1984**, *29*, 416.

(33) (a) Yokoyama, H.; Yamatera, H. *Bull. Chem. Soc. Jpn.* **1975**, *48*, 2708. (b) Pyartman, A. K.; Karmonova, E. G.; Belousov, E. A. *Russ. J. Inorg. Chem.* **1984**, *29*, 1183. (c) Pyartman, A. K.; Karmonova, E. G.; Belousov, E. A. *Russ. J. Inorg. Chem.* **1984**, *29*, 1475. (d) Pyartman, A. K.; Karmanova, E. G.; Belousov, E. A. *Russ. J. Inorg. Chem.* **1984**, *29*, 632.

(34) Yokoyama, Y.; Yamatera, H. *Bull. Chem. Soc. Jpn.* **1975**, *48*, 1770.

(35) D'Aprano, A.; Fuoss, R. M. *J. Phys. Chem.* **1969**, *73*, 400.

(36) (a) Kumar, C. V.; Barton, J. K.; Turro, N. J. *J. Am. Chem. Soc.* **1985**, *107*, 5518. (b) Barton, J. K.; Lolis, E. *J. Am. Chem. Soc.* **1985**, *107*, 708. (c) Barton, J. K.; Danishefsky, A. T.; Goldberg, J. M. *J. Am. Chem. Soc.* **1984**, *106*, 2172. (d) Barton, J. K.; Basik, L. A.; Danishefsky, A.; Alexandrescu, A. *Proc. Natl. Acad. Sci. U.S.A.* **1984**, *81*, 1961.